JOURNAL OF Materials CHEMISTRY

Strategies towards functionalised electronically conducting organic copolymers: Part 2. Copolymerisation

Karl S. Ryder,*[a] Lutz F. Schweiger,[b] Andrew Glidle[c] and Jon. M. Cooper[c]

[a]*Department of Chemistry, Hawthorn Building, De Montfort University, The Gateway, Leicester, UK LE1 9BH*
[b]*Department of Chemistry, University of Aberdeen, Meston Walk, Old Aberdeen, UK AB24 3UE*
[c]*Department of Electronics & Electrical Engineering, Rankine Building, University of Glasgow, Glasgow, UK G12 8LT*

Received 16th February 2000, Accepted 12th May 2000
Published on the Web 26th June 2000

Here we discuss the application of X-ray photoelectron spectroscopy and absorbance–reflectance FT-IR spectroscopy to establish and quantify reactivity relationships between a range of thiophene and pyrrole monomers. In particular we investigate the application of these techniques to the characterisation of conducting polymer materials grown potentiostatically from solutions containing a binary mixture of monomers. Our data have shown that XPS is especially effective in determining polymer composition and the linear correlation between this and solution composition has enabled prescriptive synthesis of copolymer materials from the different combinations of monomers described here. This technique is much more convenient and more reliable than elemental analysis. In contrast we show that FT-IR studies, whilst providing a useful qualitative guide to the functional group content of the material, do not facilitate detailed quantitative analysis because of large intrinsic errors.

1.0 Introduction

In our research we have sought routes to functionalised organic conductors as materials with potentially good electronic properties *e.g.* high conductivity, low bias voltage, and functional utility. Both academic and industrial interest in such materials continues to expand and important application growth areas include films for light emitting devices and polymer transistors for active displays and data storage, biosensors and artificial olfaction.[1,2] Our efforts have focused on the fabrication of polymer materials based on copolymers of functionalised pyrrole and thiophene units. In this approach we seek to minimise the steric interactions between adjacent functionalised repeat units in the polymer that are known to be detrimental to the electronic properties of the material *e.g.* conjugation length, conductivity.[3–7] We have adopted a two-fold strategy:

(1) Synthesis of mixed oligomeric precursors containing pyrrole and functionalised thiophene.
(2) Electrochemical copolymerisation from solutions containing a mixture of thiophene and pyrrole monomers.

The former strategy has certain advantages associated with control resulting from synthesis of discrete precursor units but is made difficult by the rigorous nature of the synthetic chemistry. This is described in an earlier paper in this journal.[8] The second strategy is attractive from a different perspective because electrochemical synthesis of copolymers from solution mixtures is experimentally facile. Additionally, the desired functionality can be incorporated into the film as either a pyrrole or thiophene derivative. The main disadvantage of this procedure is that the composition of copolymer materials produced by this technique seldom corresponds to the composition of the solution from which the material was polymerised. This reflects the disparate reactivities and oligomer solubilities of pyrrole and thiophene monomers and is problematic because characterisation of the insoluble, infusible polymer materials is difficult.† For example the composition of copolymers of pyrrole and *N*-arylpyrroles were studied using elemental analysis.[9–11] This is typical of many subsequent studies but it was concluded at an early stage that these methods, whilst both tedious and expensive, are also often unreliable. Nevertheless, many research groups have adopted this approach and their efforts have been recently summarised.[12] In cases where the component reactivities and solubilities are similar and there is no steric hindrance, *e.g.* pyrrole and *N*-methylpyrrole, the composition of the feedstock solution does mirror the make up of the copolymer; however this situation is unusual.[4,5] Other methodologies to control the composition of a copolymer grown from a particular solution mixture have been adopted, including manipulation of diffusion layer concentrations using pulsed polarography.[13] However, this latter technique still requires an implicit empirical knowledge of the reactivities of the component monomers.

Here we concentrate on the study of copolymer materials prepared electrochemically from solutions containing a binary mixture of different monomer species. The monomer species chosen for this study are good examples of functional utility where subsequent chemistry at these groups imparts useful and specific properties to the material. These studies have involved quantitative determination of polymer composition using X-ray photoelectron spectroscopy and qualitative comparisons of intensity data using absorbance–reflectance FT-IR spectroscopy. These complementary techniques have yielded an insight into the relative ability of a series of heterocyclic conducting polymer precursor compounds to form adherent copolymer films. Ultimately we seek to determine the appropriate calibration data and conditions for each monomer mixture to enable prescriptive synthesis of copolymer materials with a given composition from a particular set of monomer components. We also describe our attempts to determine the relative reactivities of several functionalised pyrrole and

†Another more subtle problem lies in the general assumption that such copolymer materials are homogeneous rather than phase separated mixtures, however, we will not address this issue here.

thiophene species by comparing the composition of polymer material, as determined using XPS, with the composition of the binary feed solution from which the polymers were electrochemically grown. In addition we have examined the absorbance–reflectance FT-IR spectra of the polymer films to determine the relative intensity of the nitrile and ester carbonyl bands of the functionalised heterocyclic species.

2.0 Experimental

2.1 General methods

Commercial reagents were used without further purification. Solvents were purified and degassed according to standard procedures. ^{1}H and ^{13}C NMR data were obtained on Varian Unity Inova 400 MHz and Bruker AC-F 250 MHz spectrometers. FT-IR spectra were recorded using a Nicolet 205 FT-IR spectrometer; polymer film spectra were recorded *ex situ* using a specular reflectance accessory at an incident angle of 45°. In order to prevent spectral baseline distortion caused by conduction band effects the polymer samples were prepared in their fully reduced form. The FT-IR spectra were analysed and integrated using the ATI Mattson WinFIRST software. Mass spectra were recorded on a Finnigan MassLab Navigator. The composition of the polymer films was examined using the Scienta ESCA 300 X-ray photoelectron spectrometer (typical slit width = 0.8 mm, take off angle = 90°) at the CCLRC RUSTI facility at Daresbury.

2.2 Monomer synthesis

Monomers **1** and **8** were obtained commercially (Aldrich) and used as supplied. Synthesis and characterisation of monomers **2**, **3**, **4**, and **5** (Fig. 1) have been described by us elsewhere.[8,14] To our best knowledge compounds **6** and **7** are new compounds and their preparation is described below.

2.2.1 Preparation of pentafluorophenyl 1*H*-pyrrole-3-butyrate, 6. Monomer **6** was prepared in four stages from *N*-phenylsulfonylpyrrole, the synthesis of which has been previously described.[15,16] These four stages consist of (***i***) Friedel–Crafts acylation with succinic anhydride to give 4-[(*N*-phenylsulfonyl)pyrrol-3-yl]-4-oxobutyric acid, (***ii***) Clemmensen reduction of the ketone group, (***iii***) cleavage of the *N*-protecting phenylsulfonyl group to give 1*H*-pyrrole-3-butyric acid and (***iv***) coupling of the free pyrrole acid with pentafluorophenol using dicyclohexylcarbodiimide. These procedures are described sequentially below.

*Preparation of 4-[(N-phenylsulfonyl)pyrrol-3-yl]-4-oxobutyric acid, (***i***).* To a suspension of $AlCl_3$ (14.67 g; 110 mmol) in 175 ml of CH_2Cl_2, succinic anhydride (5.5 g; 55 mmol) was added. This was stirred for 20 min at RT after which time all material was in solution. A solution of *N*-phenylsulfonylpyrrole (10.35 g; 50 mmol) in 25 ml of CH_2Cl_2 was then added dropwise. The resultant orange solution was stirred at RT for a further 18 h. The reaction mixture was quenched with ice and H_2O, the organics were extracted with CH_2Cl_2 (3×50 ml); the extracts were washed with brine, and dried over $MgSO_4$ and the solvent was removed under partial vacuum. The target, (***i***), was obtained as a white crystalline solid, 6.68 g (21.7 mmol; 43%); mp 124–126 °C, after recrystallisation.

*Preparation of 4-[(N-phenylsulfonyl)pyrrol-3-yl)butyric acid, (***ii***).* To a solution of (***i***) (6.68 g; 21.74 mmol) in toluene (100 ml) and H_2O (20 ml), freshly prepared amalgamated zinc was added. [Amalgamated zinc was prepared by stirring a mixture of mercuric chloride (5.02 g; 18.49 mmol) and zinc powder (48.40 g; 740 mmol) in HCl conc. (20 ml) and H_2O (100 ml) for 20 min.] The mixture was stirred for 20 min, after which more HCl (40 ml) was added. This mixture was then held at reflux for 20 h, during which 3 additional portions of HCl conc. (3×25 ml) were added. After cooling to RT the aqueous fraction was extracted with diethyl ether (3×50 ml), after which the combined organic fractions were washed with brine, then with H_2O, dried over $MgSO_4$, filtered and concentrated. The remaining orange solid was recrystallised from toluene which gave (***ii***) as a white solid, 2.99 g (10.22 mmol; 47%); mp 91–93 °C.

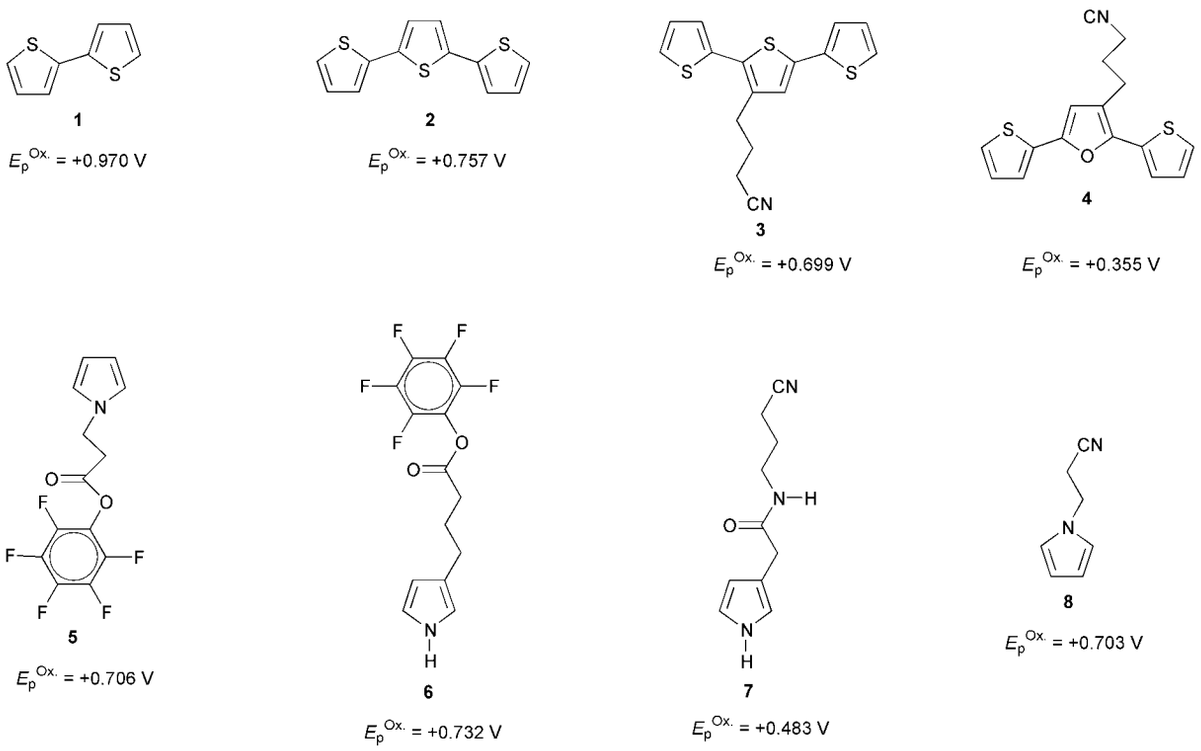

Fig. 1 Peak anodic potentials for the irreversible oxidation of species above, E_p^{Ox}, were recorded relative to the ferrocinium/ferrocene couple as an internal calibrant.

*Preparation of 1H-pyrrole-3-butyric acid, (**iii**).* A solution of (***ii***) (1.8 g; 6.1 mmol) in 25 ml of methanol was cooled to 0 °C. Then 5 M NaOH (17 ml) solution was added dropwise after which the yellow reaction mixture was held at reflux for 5 h. The methanol was removed and the green aqueous solution was cooled in an ice–H_2O bath. This solution was acidified with HCl conc. to pH 2 and the product extracted with diethyl ether (3×25 ml). Drying of the combined organic phases over Na_2SO_4, filtration and concentration gave a white solid. Recrystallisation from toluene gave (***iii***) as white crystals, 0.783 g (5.18 mmol; 85%); mp 93–94 °C.

*Preparation of pentafluorophenyl 1H-pyrrole-3-butyrate, **6**.* Monomer (***iii***) (1.12 g; 7.39 mmol), dicyclohexylcarbodiimide (DCC) (1.51 g; 7.39 mmol) and pentafluorophenol (1.36 g; 7.39 mmol) were dissolved in 35 ml of MeCN. After stirring for several minutes a dense white precipitate of dicyclohexylurea (DCU) appeared. The yellow mixture was stirred at RT for a further 18 h. The precipitate was filtered off and the solvent removed under vacuum to yield a yellow oil. Column chromatography (SiO_2, CH_2Cl_2– hexane (1 : 1) gave **6** as colourless crystals, 2.12 g (6.64 mmol; 90%); mp 38 °C.

IR(KBr): $\nu = 3368$ (N–H), 3140–3110 (C–H arom.), 2965–2909 (C–H aliph.), 1789 (C=O) cm^{-1}. ^{1}H-NMR (250 MHz; $CDCl_3$): $\delta = 2.06$ (quintet, $J = 14.9$ Hz, 2H, -CH_2-CH_2-CH_2), 2.60, 2.72 (2t, $J = 7.3$, 7.6 Hz, 4H, -CH_2-CH_2-CH_2-), 6.11 (dd, $J_{4,5} = 4.0$ Hz, $J_{4,2} = 2.4$ Hz, 1H, *H*-4), 6.61 (dd, $J_{2,4} = 2.4$ Hz, $J_{2,5} = 5.2$ Hz, 1H, *H*-2), 6.75 (dd, $J_{5,4} = 4.0$ Hz, $J_{5,2} = 5.2$ Hz, 1H, *H*-5), 8.16 (br s, 1H, N*H*).

2.2.2 Preparation of *N*-(3-cyanopropyl)-2-pyrrol-3-ylacetamide, 7. Monomer **7** was prepared by nucleophilic substitution of pentafluorophenyl 1*H*-pyrrole-3-acetate (the preparation of which is described elsewhere[17,18]) with 3-amino-*n*-butyronitrile. The latter was prepared by reductive cleavage of 3-phthalimidobutyronitrile.

*Preparation of 3-phthalimidobutyronitrile, (**v**).* A solution of potassium phthalimide (30 g; 0.16 mol) in 3-bromobutyronitrile (14.78 ml; 0.148 mol) and dry ethanol (100 ml) was heated to a gentle reflux for 18 h. The ethanol (*ca.* 50 ml) was distilled off and the residual liquid was poured into dist. H_2O (400 ml). An oil separated and solidified leaving a white solid which was collected and recrystallised from dry methanol. Subsequently, (***v***) was obtained as white crystals, 26.3 g (0.123 mol; 83%); mp 64–65 °C (lit.,[19] 65–66 °C).

IR(KBr): $\nu = 3060$ (C–H arom.), 2947–2922 (C–H aliph.), 2243 (C≡N), 1695–1615 (C=O) cm^{-1}. ^{1}H-NMR (250 MHz; $CDCl_3$): $\delta = 2.06$ (quintet, 2H, -CH_2-CH_2-CN), 2.42 (t, 2H, CH_2-CN), 3.81 (t, 2H, N-CH_2), 7.69–7.76 (m, 2H, H-5, H-6), 7.81–7.89 (m, 2H, H-4, H-7,).

*Preparation of 3-aminobutyronitrile, (**vi**).* A mixture of (***v***) (12.4 g; 0.0579 mol) and 100 ml of dry ethanol was heated to a gentle reflux until all was dissolved. Hydrazine hydrate (5.95 ml; 0.123 mol) and water (5.95 ml) were added and the mixture was stirred at RT for 15 min until a white precipitate appeared. After adding a further 50 ml of dist. H_2O and 50 ml of ethanol the white precipitate dissolved and conc. HCl was then added dropwise until pH 3.5. This mixture was then held at reflux for 3 h. A white precipitate was filtered off and the residue of the solution was concentrated down to a small volume. This was cooled to 0 °C and 50 ml of 5 M NaOH was added dropwise. The white slurry was extracted with $CHCl_3$ (3×75 ml). The combined organic fractions were dried over $MgSO_4$ and concentrated. A yellow oil was obtained and this was dissolved in 75 ml of Et_2O. Anhydrous HCl gas was then admitted and a white precipitate appeared ,which was isolated and dried. Finally 40 ml of a 10 M NaOH solution was added to the dry solid and the aqueous layer was extracted with $CHCl_3$ (3×50 ml). After drying over $MgSO_4$ and concentrating, an orange oil remained which was then distilled. 3-Aminobutyronitrile was obtained as a colourless oil, 2.25 g (0.0267 mol; 46%).

IR(film): $\nu = 2936$–2871 (C–H aliph.), 2245 (C≡N) cm^{-1}. ^{1}H-NMR (250 MHz; $CDCl_3$): $\delta = 1.72$ (quintet, 2H, -CH_2-CH_2-CH_2-), 2.41 (t, 2H, Br-CH_2-), 2.81 (t, 2H, -CH_2-CN).

Preparation of N-(3-cyanopropyl)-2-pyrrol-3-ylacetamide, 7. In the final step of this synthesis, pentafluorophenyl 1*H*-pyrrole-3-acetate (0.8 g; 2.75 mmol) and 3-aminobutyronitrile, (***vi***) (0.271 g; 3 mmol) were dissolved in THF (30 ml). This solution was then held at reflux for 18 h after which it was allowed to cool to RT. A white precipitate appeared, which was filtered off. The solvent was subsequently removed to yield a light yellow oil. Column chromatography (SiO_2, ethyl acetate–hexane (1 : 1)) gave *N*-(3-cyanopropyl)-2-pyrrol-3-ylacetamide, **7**, as colourless crystals, 0.514 g (2.69 mmol; 98%); mp 49–50 °C.

IR(KBr): $\nu = 3584$–3240 (N–H), 3084 (C–H arom.), 2935–2882 (C–H aliph.), 2247 (C≡N), 1651 (C=O) cm^{-1}. ^{1}H-NMR (250 MHz; $CDCl_3$): $\delta = 1.81$ (quintet, $J = 13.7$ Hz, 2H, CH_2-CH_2-CH_2), 2.32 (t, $J = 7.3$ Hz, 2H,-CH_2-C≡N), 3.32 (q, $J = 12.8$ Hz, $J = 6.4$ Hz, 2H, NH-CH_2), 3.47 (s, 2H, CH_2-CO), 6.09 (br s, 1H, NH), 6.11 (dd, $J_{4,2} = 2.4$ Hz, $J_{4,5} = 4.0$ Hz, 1H, *H*-4), 6,76 (dd, $J_{5,4} = 4.0$ Hz, $J_{5,2} = 4.9$ Hz, 1H, *H*-5), 6.81 (dd, $J_{2,4} = 2.4$ Hz, $J_{2,5} = 4.9$ Hz, 1H, *H*-2), 8.32 (br s, 1H, N-*H*). ^{13}C-NMR (250 MHz; $CDCl_3$): $\delta = 14.77$ (CH_2-*C*H_2-CH_2), 25.58 (CH_2-*C*H_2-C≡N), 35.14 (*C*H_2-CO), 38.25 (NH-*C*H_2), 109.28 (*C*≡N-), 116.13, 117.34 (*C*-2,5), 119.17, 119.29 (*C*-3,4), 172.94 (*C*=O).

2.3 Electrochemical methods

Copolymer materials were polymerised under potentiostatic control from binary monomer mixtures on Au coated glass electrodes (*ca.* 1 cm^2) from acetonitrile solutions using 0.1 M [NBu_4][ClO_4]or 0.1 M [NBu_4][BF_4] as a supporting electrolyte. The concentration of the minority component of the mixture (typically the pyrrole) was in the range 5–20 mM whilst that of the majority component was scaled according to the specific mol ratio (see Results and discussion). The polymerisation potential was set in the range 200–250 mV positive of the foot of the wave for the monomer with the most anodic process. Thus it was ensured that the polymerisation reaction proceeded under diffusion control. All solutions were thoroughly degassed with Ar prior to polymerisation. Subsequent to polymer growth, samples were examined using absorbance–reflectance FT-IR and cyclic voltammetry. All electrochemical procedures were carried out using an E.G. & G. M263A potentiostat/galvanostat driven by the M270 software package.

3.0 Results and discussion

The experiments described in this manuscript comprise firstly anodic electrochemical (potentiostatic) growth of copolymer (on a gold coated glass slide in 0.1 M [NBu_4][ClO_4] or [NBu_4][BF_4] in MeCN) from a solution containing a binary mixture of monomers, **A** and **B,** followed by analysis of the copolymer films using absorbance–reflectance FT-IR and X-ray photoelectron spectroscopies. A number of polymers were grown for each binary mixture covering a wide range of solution compositions. The polymer materials were characterised in terms of the ratio of **A** and **B** units within the material by integrating the relative intensities of the S(2p) and F(1s) regions of the X-ray photoelectron spectrum unique to each monomer. It is an important feature of these experiments that the oxidation potential for all the copolymerisation reactions was chosen so that both monomers of the mixture were reacting at the electrode under diffusion controlled conditions. This was

achieved by poising the applied potential at a value at least 200 mV positive of the most anodic peak potential. Consequently the composition of the copolymer materials was determined by the relative reactivities of the oxidised monomer species rather than by the difference in their redox potentials. For each set of experiments, homopolymers of both species, **A** and **B**, were separately prepared using the value of applied potential corresponding to that employed for the preparation of the copolymer samples. In each case facile homopolymer growth was observed indicating that the conditions for copolymer formation were not sufficient to cause overoxidation of the species with the least anodic redox potential. In these experiments it is certainly the case that the intrinsic reactivity of the radical species is not the only influence that governs how rapidly that species is incorporated into a copolymer film. For example solubility of small oligomers or larger species will affect the composition of the solid. In this work we have not sought to characterise the soluble products of oxidation, rather we have applied the term *reactivity* to a solution species in respect of the propensity for that species to be incorporated into a solid adherent polymer film.

The thiophene and pyrrole species selected for this study are shown in Fig. 1, and represent a sample of novel tricyclic mixed derivatives, **3** and **4**, functionalised pyrrole monomers, **5**, **6**, **7**, **8** and commercially available thiophene systems **1** and **2**. The peak potentials for the irreversible anodic oxidations are also presented for completeness. In particular, the pentafluorophenoxy group of **5** and **6** whilst facilitating subsequent functional group chemistry at the carbonyl group of these molecules,[14,18] also acts as a spectroscopic label for XPS determination. This is because F has a high sensitivity for XPS measurements.[20] Additionally, the nitrile and carbonyl stretching bands of species **3**–**8** provide scope for qualitative comparison by observation of the relative intensity of these bands in copolymers fabricated from solution mixtures at different compositions.

3.1 Analysis of copolymers using XPS

Fig. 2 shows a series of X-ray photoelectron spectra in the F(1s) region for a range of copolymers grown from solution mixtures of monomers **A**=**1** and **B**=**5**, Table 1. This series of spectra shows two important features. Firstly, the presence of the F(1s) line in the spectrum is evidence of the presence of **B** in the polymer film, as is the presence of a N(1s) signal in the lower binding energy region. Second, the relative amount of this unit in the copolymer, evidenced by the intensity of the F(1s) signal, decreases as the proportion of the other component, **A** (monomer **1**, 2,2′-bithiophene) in the feed solution is increased.‡ This behaviour is mirrored by the intensities of the corresponding signals in the S(2p) spectral region for the same polymer samples, Fig. 3, *i.e.* the S(2p) intensity increases with the proportion of bithiophene, **A**=**1**, in the film. Since **B** (monomer **5**) contains no sulfur atoms and, similarly, **A** (monomer **1**, 2,2′-bithiophene) contains no fluorine atoms, quantitative elemental analysis of the copolymer films is facilitated by the weighted ratio of the two spectral regions (taking the appropriate elemental spectral sensitivity factors into account). The composition of these copolymers, in terms of their **A** and **B** components, calculated thus are presented in Table 1. From these data it is clear that the bithiophene, **1**, is incorporated into the film during electropolymerisation, much more slowly than is the pyrrole ester, **5**. For example the polymer that was produced from a solution containing 25 mol of bithiophene, **1**, to 1 mol pyrrole ester, **5**, contains only 1.8 units of bithiophene for every pyrrole moiety, Table 1. This is not surprising since, to our knowledge, there are very few examples of copolymers grown from pyrrole–thiophene mixtures that proportionately reflect the composition of the feedstock solution. In one such case the powder material was prepared but only using $FeCl_3$ as a chemical oxidant.[21]

The data presented in Table 1, and in subsequent Fig. 4 and 5, are characterised by a reasonably good linear correlation between the solution composition and the resultant polymer composition. Consequently the composition of a given polymer sample can be determined from a knowledge of the solution composition and the linear scaling factor that is related to the relative reactivities of the two monomers *i.e.* the gradient. For example if the two components of the mixture were of similar reactivity then the composition of the polymer would be the

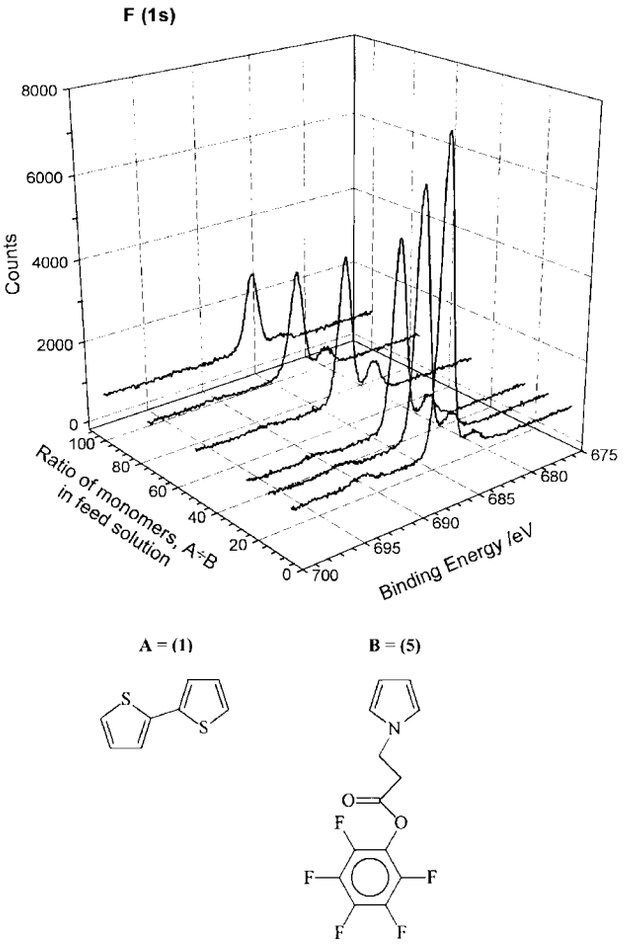

Fig. 2 XPS, F(1s) region of series of copolymers grown from solution mixtures containing **A**=**1** and **B**=**5** in ratios (A : B); 100 : 1, 75 : 1, 50 : 1, 25 : 1, 15 : 1, and 5 : 1. Thin film sample (*ca.* 0.5 μm) supported on a Au coated SiO_2 electrode recorded using a slit width of 0.8 mm and a take off angle of 90°.

Table 1 Correlation of solution and copolymer composition expressed as mol ratio

Mol ratio, **A** : **B**, of monomers in feed solution **A**=**1**, **B**=**5**	Mol ratio, **A** : **B**, of components in the copolymer
100 : 1	7.1
75 : 1	4.1
50 : 1	2.3
25 : 1	1.8
15 : 1	1.1
5 : 1	0.5

‡Best polymer growth for this experiment was achieved using $[NBu_4][BF_4]$ as supporting electrolyte. Consequently the F(1s) spectra in Fig. 2 show a low binding energy feature corresponding to small amounts of BF_4^- ion. These features were excluded from our quantitative analysis by deconvolution from the main F(1s) signal using the Scienta WinEsca spectral manipulation software.

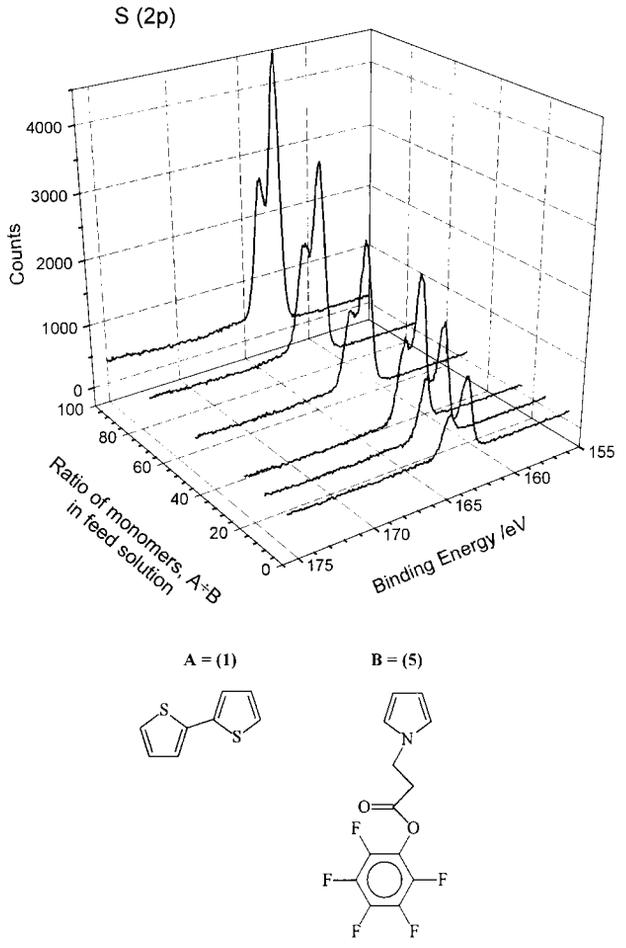

Fig. 3 XPS, S(2p) region of series of copolymers (same samples as Fig. 2) grown from solution mixtures containing **A**=**1** and **B**=**5** in ratios (A : B); 100 : 1, 75 : 1, 50 : 1, 25 : 1, 15 : 1, and 5 : 1. Thin film sample (*ca.* 0.5 μm) supported on a Au coated SiO_2 electrode recorded using a slit width of 0.8 mm and a take off angle of 90°.

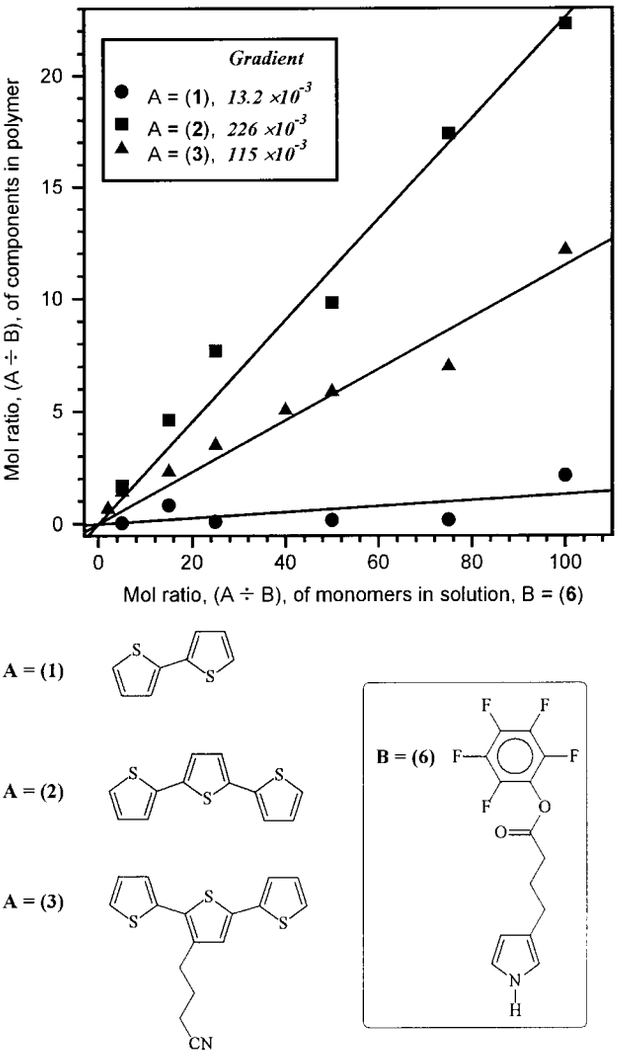

Fig. 4 Composition of a range copolymers (determined from integration of the F(1s) and S(2p) regions of the XPS spectra), in terms of component ratio (**A**=**1**, **2**, or **3**: **B**=**6**), *versus* composition of polymerisation solution. The gradients of the linear regressions are **1** ● = 13.2×10^{-3}, **2** = 226×10^{-3} and **3** ▲ = 115×10^{-3}.

same as that of the solution from which the polymer was formed and so the corresponding gradient would be unity. However, the gradients of the plots in Fig. 4 and 5 show very disparate reactivities for the species investigated here, *e.g.* bithiophene **1** is very much less reactive than the pyrrole ester **5**, under these reaction conditions.

The results from a series of experiments using feed solutions with different binary combinations are presented in Fig. 4. In these experiments the pyrrole component of the mixture was monomer **6**, in combination with three different thiophene species **1**, **2**, or **3**. The gradients for the linear correlations of these data are presented in Table 2. Apparent from this plot is that the thiophene component is in all cases very much less reactive than the pyrrole component. For example, the copolymer grown from a solution containing a 100 : 1 mol ratio mixture of molecules **1** and **6**, Fig. 4 (●), consists of a mixture of the same units in a 2 : 1 ratio. In other words there is proportionately 30 times more pyrrole in the copolymer than there was in solution. However, the copolymers fabricated from solution mixtures containing molecules **2** and **6**, Fig. 4 (■), show a much greater proportion of thiophene units in the copolymer at similar feed solution ratios indicating that terthiophene, **2**, is more reactive than bithiophene, **1**, under these conditions. Intermediate to the behaviour of the species **1** and **2** is that of species **3**, Fig. 4 (▲). This novel functionalised terthiophene is evidently less reactive than unsubstituted terthiophene presumably because of steric effects resulting from the cyanoalkyl substituent or because its oligomers are more soluble.

The results from another series of similar experiments are presented in Fig. 5. In these experiments the pyrrole component of the mixture was monomer **5**, in combination with species **1**, **2**, **3** or **4**. The linear correlations for this data set whilst less good than those in Fig. 4, nevertheless show a clear trend of reactivities. For the experiment where copolymers were grown from a solution containing a mixture of **2** and **5** [Fig. 5, (■)] correlation has resulted in a line of linear regression (dotted line) that deviates markedly from the real origin. An intercept in these plots has no physical significance, as a solution ratio, **A** : **B,** of zero represents pure **B**, where in this example **B**=**5**. Consequently the observed intercept in Fig. 5 is likely to be due to experimental error in the polymer analysis.§

The gradients from Fig. 4 and Fig. 5 are collected together in Table 2. From these gradients the order of relative reactivity is mutually consistent and is summarised as follows; **2**>**4**>**3**>**1**, where terthiophene is the most reactive and bithiophene is the least reactive. This is consistent with the observations of other groups in that terthiophenes are generally regarded as more reactive than bithiophenes which are, in turn, more reactive

§Constraining the linear regression of these data to a real origin nevertheless results in a significantly increased gradient and so the value that appears on Fig. 6, and in Table 2 represents a minimum estimate. The additional error introduced by this constraint, however, does not alter the order of reactivity of the molecules in this series.

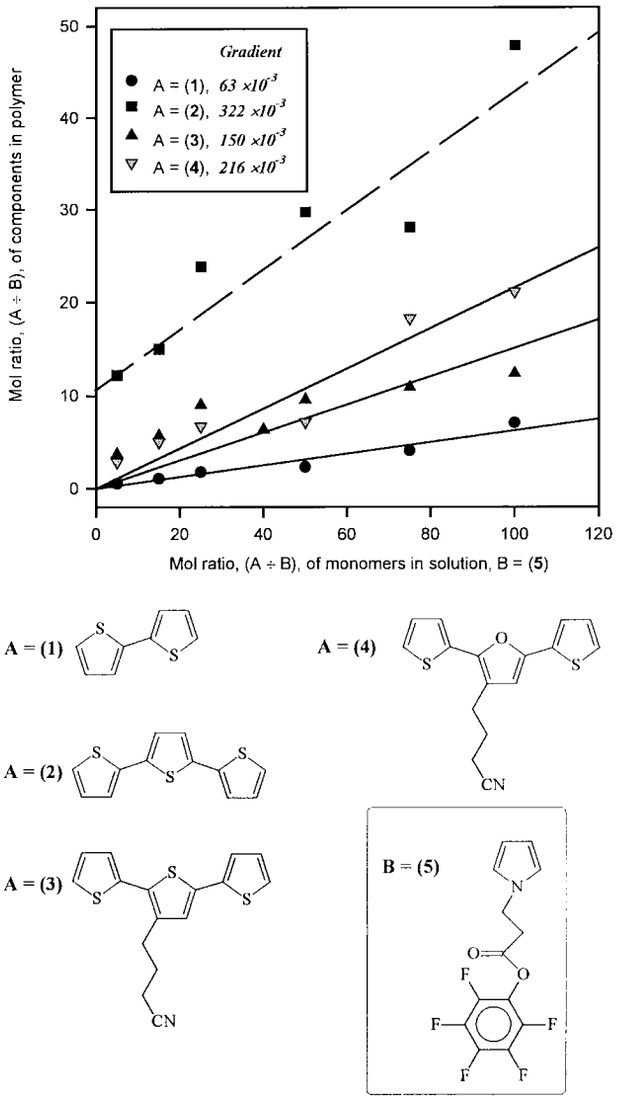

Fig. 5 Composition of a range of copolymers (determined from integration of the F(1s) and S(2p) regions of the XPS spectra), in terms of component ratio (**A**=**1**, **2**, **3**, or **4**: **B**=**5**), *versus* composition of polymerisation solution. The gradients of the linear regressions are **1** ●$=63\times10^{-3}$, **2** ■$=322\times10^{-3}$, **3** ▲$=150(80)\times10^{-3}$ and **4** ▼$=216\times10^{-3}$. [N.B. The data set labeled ● corresponds to that presented in Table 1].

than thiophene monomers towards film formation.[2] Furthermore, the effect of the cyanoalkyl substituent in **3** and **4** is likely to be steric as is observed in other pyrrole and thiophene systems.[7,12] In addition, comparison of like data sets from Fig. 4 and Fig. 5, for example; {**A**=**1**+**B**=**6**}, Fig. 4 (●), with {**A**=**1**+**B**=**5**}, Fig. 5 (●), or, alternatively, {**A**=**2**+**B**=**6**}, Fig. 4 (■), with {**A**=**2**+**B**=**5**}, Fig. 5 (■), reveal that the gradients are consistently and considerably larger in the experiments where the pyrrole component, **B**, is the *N*-substituted pyrrole ester **5**. Since a larger gradient is indicative of a larger thiophene content we can conclude that the β-substituted pyrrole ester, **6**, is more reactive in combination with these thiophene systems than is the *N*-substituted pyrrole ester **5**. Consequently the overall reactivity order for this series of compounds with respect to the formation of coherent, adhesive films is as follows; **6**>**5**≫**2**>**4**>**3**>**1**. Interestingly this reactivity order bears little resemblance to the order of peak redox potentials, presented in Fig. 1, for these compounds. This is because the redox potential of the molecular species provides information only about how that species reacts with the electrode surface. It does not provide information about the rate of reaction between one radical cation and another dissimilar species. For example we can consider an imaginary binary mixture of species **A** and **B**, in equimolar proportions where the species have oxidation potentials of +0.5 V and +1.0 V respectively. If the copolymerisation experiments were carried out at an applied potential of +1.05 V then we might reasonably expect to obtain a copolymer that contains more **A** than **B**. This is not necessarily because of the relative intrinsic reactivities of the **A** and **B** radical cations (about which we know nothing), but simply because the overpotential for the generation of $\mathbf{A}^{+\cdot}$ is much larger than that for generation of $\mathbf{B}^{+\cdot}$, *i.e.* the concentration [$\mathbf{A}^{+\cdot}$] at the electrode surface is much larger than the concentration [$\mathbf{B}^{+\cdot}$]. Consequently, the extent to which each monomer, of the binary mixture, is incorporated into a copolymer is unlikely to correlate with the oxidation potential unless one or both of the reactions is under kinetic (potential) control. In this case the composition of copolymer is entirely dependent on the arbitrary choice of applied electrode potential. Our experiments specifically exclude this condition because, by imposing mass transport control, the reactivity of both solution species with the electrode surface is very rapid hence the composition of polymer is independent of applied potential.

Table 2 Summary of gradient data from the linear correlations in Fig. 4 and Fig. 5

Monomer A	Monomer B=5 Gradient $\times10^3$ (Fig. 5)	Monomer B=6 Gradient $\times10^3$ (Fig. 4)
1	63	13.2
2	322	226
3	150	115
4	216	—

These arguments are illustrated in this study by consideration of the combinations of **3** or **4** with **5**, Fig. 5. In the first case, (**3**+**5**), the oxidation potentials are very similar, whilst in the latter case, (**4**+**5**), the thiophene system has a redox potential 0.351 V less anodic than the pyrrole species, **5**, with which it is combined. In both cases the pyrrole component is shown to be more reactive, where, presumably, the solubility of oligomeric species is very similar.

Finally, in this analysis, we can make quantitative comparisons of the relative reactivities of the thiophene systems in the two experimental situations shown in Fig. 4 and Fig. 5. For example the ratio of gradients for the bithiophene, **1**, and terthiophene, **2**, in combination with β-pyrrole ester **6**, Fig. 4, reveals that terthiophene is >17 times more reactive than bithiophene. Similarly terthiophene, **2**, is just under twice as reactive as the substituted terthiophene, **3**, under the same conditions. In contrast, terthiophene is only five times more reactive than bithiophene when in combination with the *N*-pyrrole ester, **5**, Fig. 5. Consequently, although the β-pyrrole ester, **6**, is more likely to react with itself when in combination with any of the thiophenes of the binary mixtures in this study, nevertheless, its reactions with these thiophenes are more selective with respect to film formation, than are those of the *N*-substituted pyrrole ester **5**. It is also interesting to note the effect of substituting the S atom of **3** for O in the dithienylfuran derivative, **4**. Presumably the greater reactivity of **4** compared to that of **3** is entirely electronic in origin since the steric constraints and solubility for both molecules are very similar.

3.2 Analysis of copolymers using reflectance FT-IR

Copolymer materials grown from binary solution mixtures, in the manner described above, were also examined using absorbance–reflectance FT-IR spectroscopy. In this experiment the incident IR beam was oriented at 45° from the plane of the polymer coated electrode. The polymers were grown on gold coated glass slides such that the IR beam path length, *l*,

Table 3 Summary of FT-IR intensity data and solution composition

Mol ratio, (**A** : **B**), of monomers in solution	Integrated intensity ratio, $\nu(C\equiv N)/\nu(C=O)_{ester}$, from polymer spectra			
	A=**7**, **B**=**5** $(C\equiv N)/(C=O)_{ester}$	**A**=**7**, **B**=**6** $(C\equiv N)/(C=O)_{ester}$	**A**=**8**, **B**=**5** $(C\equiv N)/(C=O)_{ester}$	**A**=**8**, **B**=**6** $(C\equiv N)/(C=O)_{ester}$
30 : 1	5.36	0.67	—	—
25 : 1	2.38	0.48	10.0	0.67
20 : 1	1.43	0.24	10.0	0.29
18 : 1	1.61	0.26	—	—
16 : 1	0.90	—	5.00	0.11
15 : 1	—	0.17	—	—
14 : 1	1.21	—	—	0.08
12 : 1	0.91	0.17	—	—
10 : 1	—	0.10	—	0.04
8 : 1	0.90	—	1.11	—
5 : 1	—	0.09	—	—
4 : 1	0.23	—	0.53	—
2 : 1	0.13	—	0.15	—
1 : 1	0.11	—	0.06	—

through the polymer is defined as $l=2d/\sin(45^\circ)=2.83d$ where d is the film thickness.

Monomers, **5**, **6**, **7** and **8**, were selected for these experiments because they possess clearly defined, well spaced, stretching bands ascribed to the carbonyl and nitrile functionalities. For each copolymer sample the integrated intensities of the relevant carbonyl and nitrile stretching bands were ratioed and compared with the composition of the solution from which the sample was prepared. The data for a series of experiments at various solution compositions are presented in Table 3 and Fig. 6. Although these data do not provide a quantitative determination of the copolymer composition they nevertheless clearly show that under these experimental conditions the β-pyrrole ester, **6**, is incorporated into the copolymer more rapidly than is the *N*-substituted pyrrole derivative, **5**. Whilst this result is in agreement with our findings from the XPS experiments the linear regressions for these data are relatively poor because of intrinsic error.

In an attempt to quantify these errors a second series of experiments was undertaken using monomers **6** and **7**. A series of copolymers prepared from these two monomers was grown

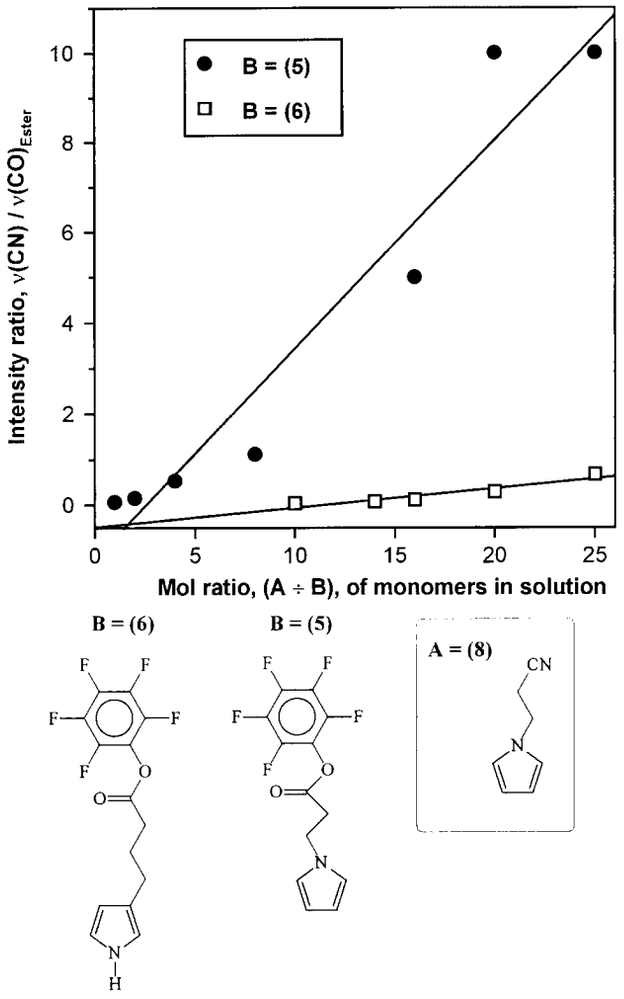

Fig. 6 Integrated intensity ratio of the $(CO)_{ester}$ and (CN) stretching bands from the FT-IR spectra of the copolymer materials plotted against the composition of the polymerisation solution, where **A**=**8** and **B**=**5** or **6**.

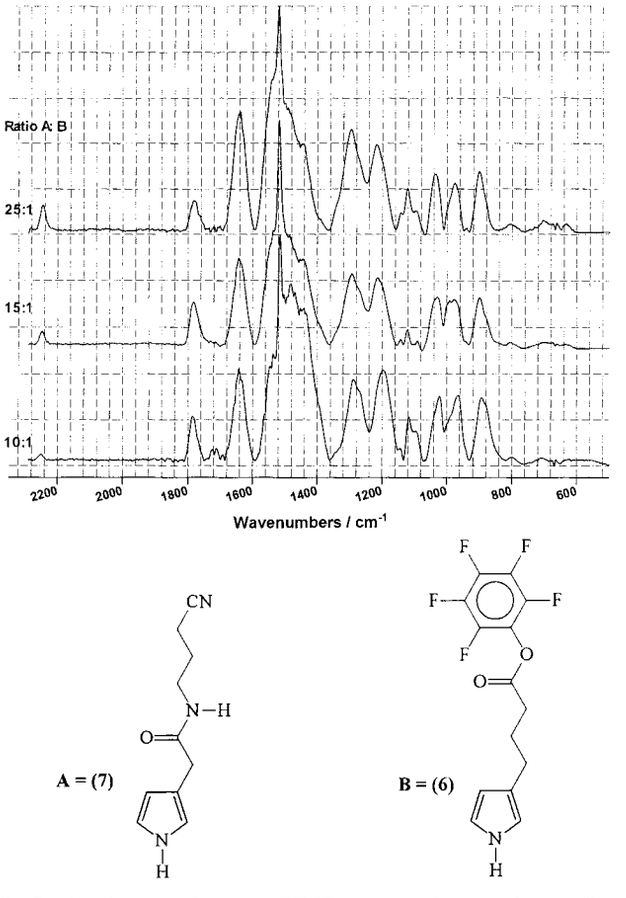

Fig. 7 Absorbance–reflectance FT-IR spectra for copolymer films grown on a Au coated glass slide from solution mixtures of monomers **A**=**7** and **B**=**6** in the ratios 10 : 1, 15 : 1 and 25 : 1 respectively. The spectra were recorded at a resolution of 4 cm^{-1} and have been baseline corrected, normalised and offset to facilitate overlay comparison.

and three representative copolymer spectra are shown in Fig. 7. Intrinsic to these spectra are the nitrile and carbonyl (amide) stretches of **7** at 2246 cm^{-1} and 1642 cm^{-1} respectively, and the carbonyl (ester) stretch of **6**, at 1782 cm^{-1}. Furthermore, as the proportion of monomer **7** in the solution is increased from 10 : 1 to 25 : 1, the concomitant increase in the relative intensity of the nitrile stretch compared with the carbonyl (ester) stretch in the copolymer spectra is clearly visible. The intensity ratio data (with appropriate error bars) and solution compositions for the full series are plotted in Fig. 8. The error bars presented in Fig. 8 represent the variation in the repeat determination of the same ratio from a given spectrum. The large error associated with the data point at the solution ratio 30 : 1 is probably caused by high noise levels in this spectrum.

The dual functionality of **7** allows internal calibration of these data since the intensity ratio of the nitrile stretch and the carbonyl (amide) stretch should be constant regardless of the polymer composition. This calibration ratio was determined from the spectrum of each copolymer in this series and the data are plotted in the insert to Fig. 8. Whilst the trend of the main graph in Fig. 8 is intuitive the insert shows that the calibration ratio varies by almost a factor of three. This result, whilst precluding any further detailed analysis of the FT-IR data gathered here, may reflect the presence of some degree of order

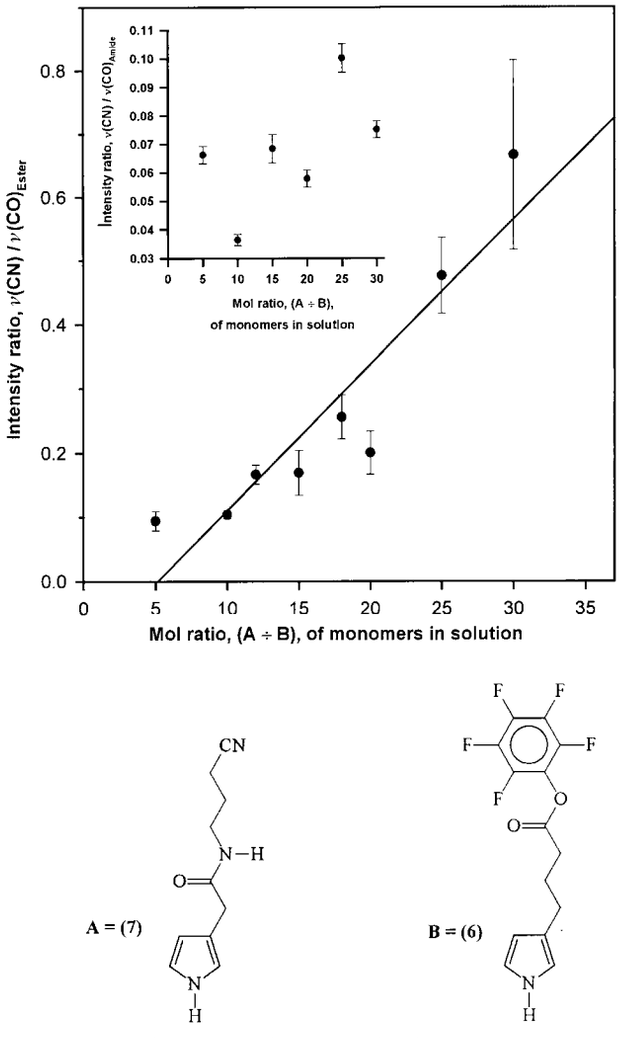

Fig. 8 *Main graph*: Integrated intensity ratio of the $(CO)_{ester}$ and (CN) stretching bands from the FT-IR spectra of the copolymer materials plotted against the composition of the polymerisation solution, where **A** = **7** and **B** = **6**. *Insert*: Integrated intensity ratio of the $(CO)_{amide}$ and (CN) stretching bands (both due to component **7** from the FT-IR spectra of the copolymer materials plotted against the composition of the polymerisation solution as above.

within the copolymer films such that the discrete IR chromophores in the polymer lie within regions at different orientations with respect to each other and with respect to the incident IR radiation. Alternatively, variation in levels or aerobic oxidation in samples and between samples might contribute to small changes of relative intensity between adjacent bands as has been observed in other systems.[22]

4.0 Conclusions

In this study we have used FT-IR and XPS techniques to establish qualitative and quantitative data regarding the relative film forming reactivities of thiophene and pyrrole species in binary combinations. Our observations are largely consistent with those of others in that the thiophene species are generally incorporated into copolymers in lower proportions than are the pyrrole species (under diffusion controlled electrochemical synthesis) and also the terthiophene derivatives are more reactive than their lower order homologues. In particular the XPS data have allowed the elucidation of a quantitative reactivity order of the monomers in this study and the linear correlation between solution composition and copolymer composition enables prescriptive synthesis of copolymer materials of a given composition from a given solution mixture. This is important because prescriptive determination of function, composition and properties such as conductivity are essential for device applications. In contrast, the FT-IR data whilst providing qualitative corroboration of the XPS analysis and conformation of functional group content, do not facilitate a detailed analysis of these materials. This is because internal calibration of the polymer spectra shows the intensity ratio data to be highly variable and therefore unreliable. Although the errors associated with integrated intensity measurements from noisy spectra were quite substantial the latter problem may be more closely associated with the internal microstructure of the copolymer materials implying regions or localised order or phase separation. In addition, variations in aerobic dopant levels might also contribute to these errors.

Acknowledgements

The authors are gratefully indebted to Dr D. G. Morris (University of Glasgow) and to Dr G. Beamson (RUSTI, Daresbury Lab.) for insight and helpful discussion, also to the University of Aberdeen, the Royal Society (RSRG17906), and the EPSRC (GR/L10185), EPSRC (CCLRC RUSTI RG168, RG213) for financial support.

References

1 R. H. Friend, R. W. Gymer, A. B. Holmes, J. H. Burroughes, R. N. Marks, C. Taliani, D. D. C. Bradley, D. A. Dos Santos, J. L. Brédas, M. Löglund and W. R. Salaneck, *Nature (London)*, 1999, **397**, 121.
2 *Handbook of Conducting Polymers*, 2nd edn., ed. T. A. Skotheim, R. L. Elsenbaumer and J. R. Reynolds, Marcel Dekker, New York, 1998.
3 G. Zotti, S. Martina, G. Wegner and A. D. Schluter, *Adv. Mater.*, 1992, **4**, 798.
4 K. K. Kanazawa, A. F. Diaz, M. F. Diaz, M. T. Krounbi and G. B. Street, *Synth. Met.*, 1981, **4**, 119.
5 O. Inganas, B. Liedberg, W. R. Wu and H. Wynberg, *Synth. Met.*, 1985, **11**, 239.
6 Y. Chen, C. T. Imrie, J. M. Cooper, A. Glidle, D. G. Morris and K. S. Ryder, *Polymer Int.*, 1998, **47**, 43.
7 J. P. Ferraris and M. D. Newton, *Polymer*, 1992, **32**, 391.
8 L. Schweiger, A. Glidle, D. G. Morris, J. M. Cooper and K. S. Ryder, *J. Mater. Chem.*, 2000, **10**(1), 107.
9 M. V. Rosenthal, T. A. Skotheim, C. Linkous and M. I. Florit, *Polym. Prepr. (Am. Chem. Soc., Div. Polym. Chem.)*, 1984, **25**, 258.

10 J. R. Reynolds, P. A. Poropatic and R. L. Toyooka, *Synth. Met.*, 1987, **18**, 95.
11 J. R. Reynolds, P. A. Poropatic and R. L. Toyooka, *Macromolecules*, 1987, **20**, 958.
12 J. P. Ferraris and D. J. Guerrero, in *Handbook of Conducting Polymers*, 2nd edn., ed. T. A. Skotheim, R. L. Elsenbaumer and J. R. Reynolds, Marcel Dekker, New York, 1998.
13 W. Schuhmann, C. Kranz, H. Wohlschlager and J. Strohmeier, *Biosens. Bioelectron.*, 1997, **12**(12), 1157.
14 C. J. Pickett and K. S. Ryder, *J. Chem. Soc., Dalton Trans.*, 1994, 2128.
15 J. Rokach, P. Hamel and M. Kakushima, *Tetrahedron Lett.*, 1981, **22**(49), 4901.
16 M. Kakushima, P. Hamel, R. Frenette and J. Rokache, *J. Org. Chem.*, 1983, **48**, 3214.
17 K. S. Ryder, D. G. Morris and J. M. Cooper, *Langmuir*, 1996, **12**(23), 5681.
18 K. S. Ryder, D. G. Morris and J. M. Cooper, *J. Chem. Soc., Chem. Commun.*, 1995, 1471.
19 A. A. Goldberg and W. Kelly, *J. Chem. Soc*, 1947, 1369.
20 G. Beamson and D. Briggs, *High Resolution XPS of Organic Polymers. The SCIENTA 300 Database*, Wiley, New York, 1992.
21 S.-A. Chen and J.-M. Ni, *Macromolecules*, 1993, **26**, 3230.
22 P. A. Christensen, A. Hamnett, A. R. Hillman, M. F. Swann and S. J. Higgins, *J. Chem. Soc., Faraday Trans.*, 1992, **38**, 595.